Recyclable microcellular rubber foams and superior photothermal performance via constructing Fe^{3+} heterodentate coordination between epoxidized natural rubber and polyaniline

Jingyi Zhu [a, b], Yukun Chen [a], Patrick Lee [c], Shuidong Zhang [a, d*1]

[a] *Institute of Emergent Elastomers, College of Mechanical and Automotive, South China University of Technology, Guangzhou 510640, China*

[b] *State Key Laboratory of Metastable Materials Science and Technology, and School of Materials Science and Engineering, Yanshan University, Qinhuangdao, Hebei 066004, China*

[c] *Multifunctional Composites Manufacturing Laboratory (MCML), Department of Mechanical and Industrial Engineering, University of Toronto, Toronto M5S 3G8, Canada*

[d] *Guangdong Key Laboratory of Technique and Equipment for Macromolecular Advanced Manufacturing, South China University of Technology, Guangzhou, 510640, China.*

Characterization of hydrogen bond interaction

The presence of hydrogen bond interaction between ENR and PANI was confirmed by comparing the spectra of ENR with EP0 in Figure 1(a). After adding PANI to ENR, the peaks associated with epoxy groups of ENR shifted to 1247 and 867 cm^{-1}, respectively. Furthermore, temperature-dependent FTIR spectra provided additional

[1] Corresponding author: Prof. Shuidong Zhang. Fax: +86 20 87110029. E-mail address: starch@scut.edu.cn

evidence for the existence of hydrogen bonds in EPx (Figure S1). It was noteworthy that the peaks at 1242 and 866 cm^{-1} (epoxy groups) exhibited blue shifts when heated from 40 °C to 90 °C, indicating the disruption and subsequent regeneration of hydrogen bonds associated with epoxy groups.[1]

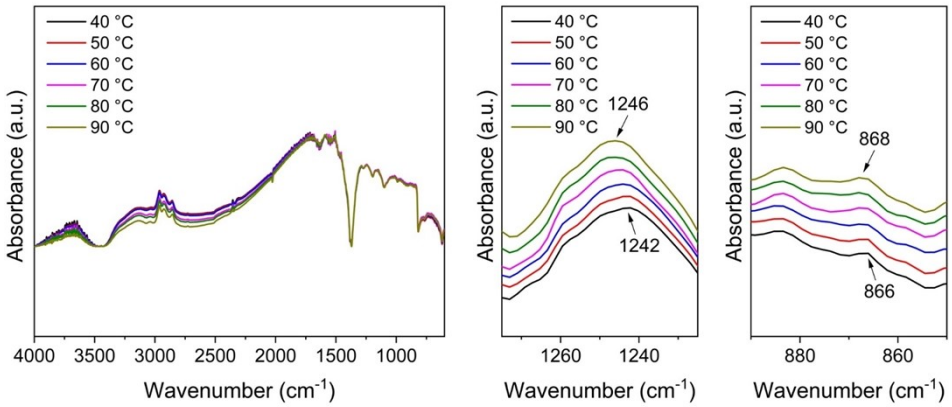

Figure S1. Temperature-dependent FTIR spectra of EP6

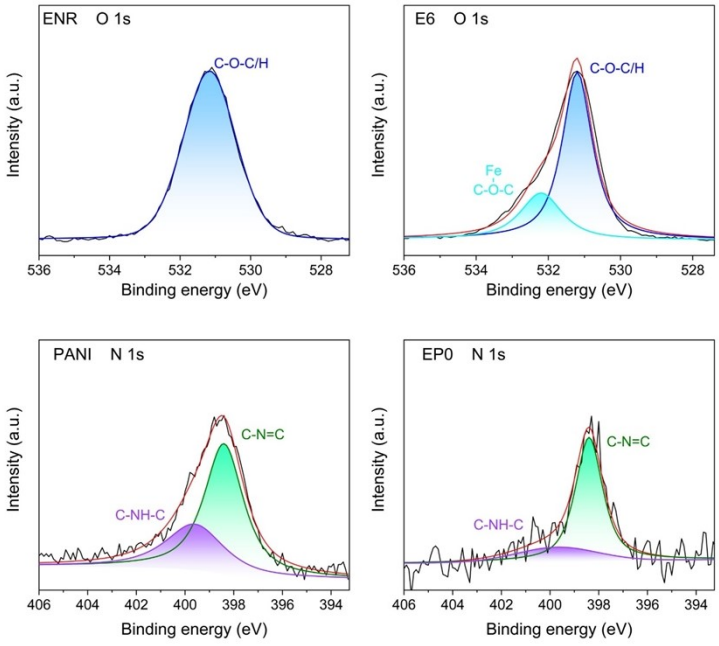

Figure S2. XPS spectra of ENR, E6, PANI and EP0

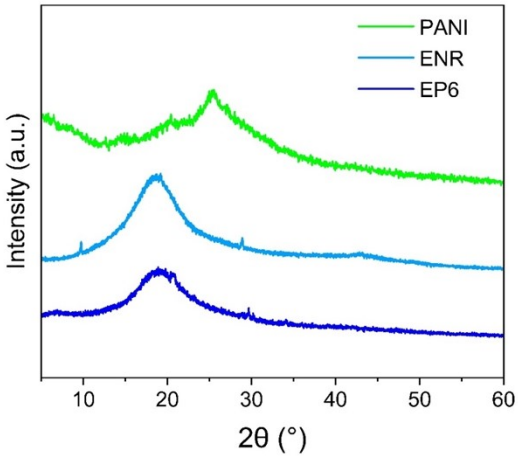

Figure S3. XRD spectra of PANI, ENR and EP6

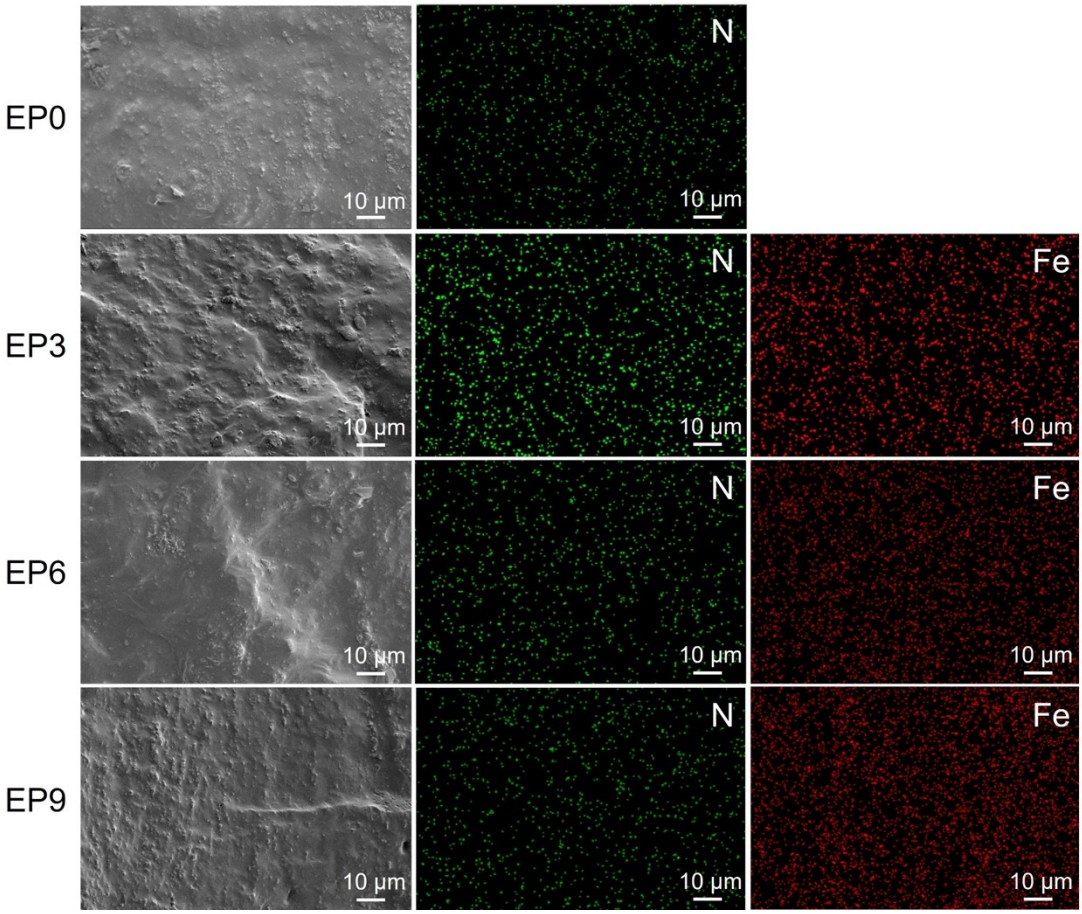

Figure S4. SEM and EDS images of EPx

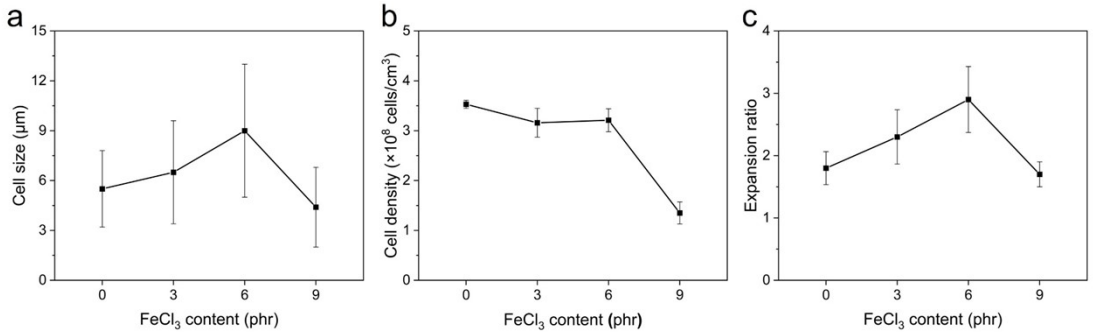

Figure S5. (a) Cell size, (b) cell density and (c) expansion ratio of f-EPx

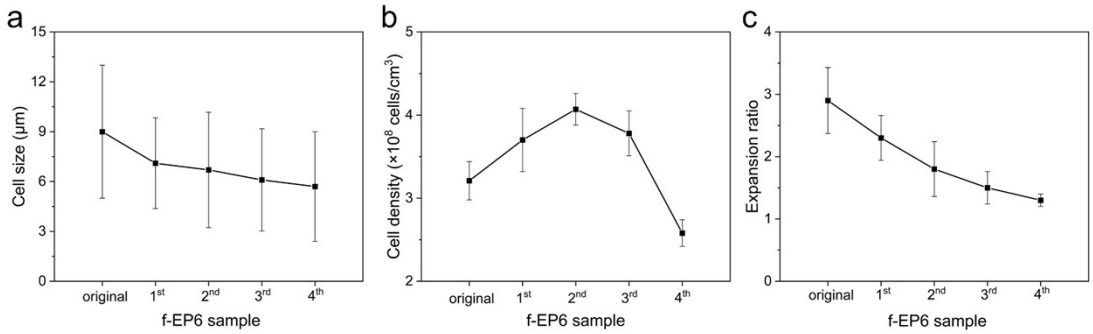

Figure S6. (a) Cell size, (b) cell density and (c) expansion ratio of original and reprocessed f-EP6

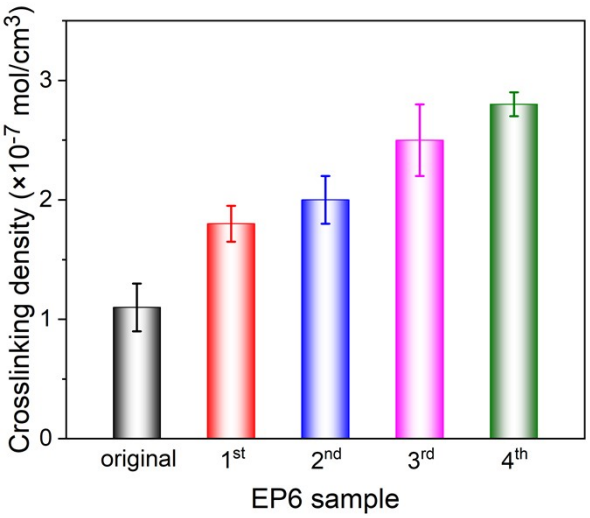

Figure S7. Crosslinking density of original and reprocessed EP6

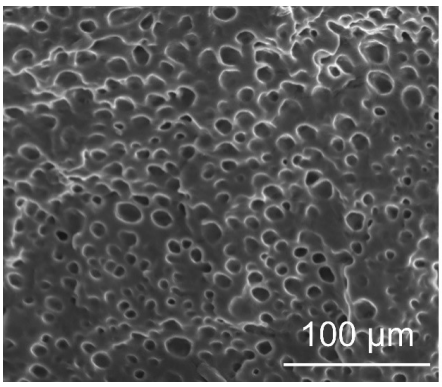

Figure S8. Cell morphology of f-EP6 after five lighting-cooling cycles

The tensile properties of EP6, f-EP6 and f-ED (crosslinking agent: DCP) were shown in Figure S9. The tensile strength and elongation at break of f-ED were 1.04 MPa and 486%, respectively. The tensile strength and elongation at break of f-EP6 were 1.61 MPa and 613%, respectively. These data demonstrated that non-covalent crosslinked rubber (f-EP6: hydrogen bond and Fe^{3+} heterodentate coordination) could also be successfully foamed like covalent crosslinked rubber (f-ED), while possessing stable cell structures and excellent mechanical properties. The higher tensile strength and elongation at break of f-EP6 could be attributed to the reinforcing effect of PANI, $FeCl_3$ and the non-covalent crosslinking structure. For solid EP6 (without cell), the tensile strength and elongation at break were 1.92 MPa and 661%, respectively. After foaming, the introduced cells may act as micro-defects, leading to stress concentration and promoting crack initiation, thus slightly reducing the tensile properties of f-EP6 compared with EP6.[2] However, due to the complete and uniform microcellular structure, the mechanical properties of f-EP6 did not deteriorate significantly and remained at a relatively high level.

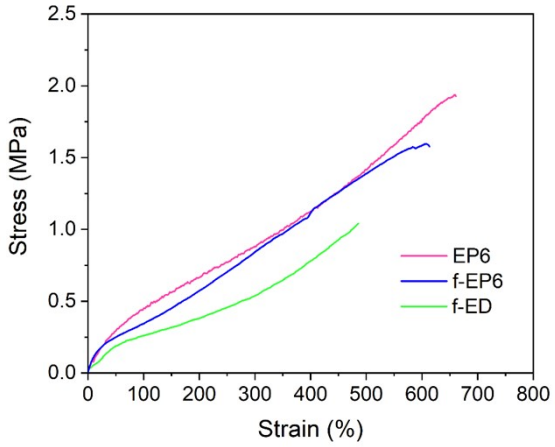

Figure S9 Tensile stress-strain curves of EP6, f-EP6 and f-ED

Calculation of photothermal conversion efficiency

Photothermal conversion efficiency was calculated based on cooling curve in Figure 7(c). Due to the energy balance of the system:[3]

$$\sum_i m_i C_{pi} \frac{dT}{dt} = Q_s - Q_{loss} \tag{S1}$$

where m and C_p are the mass (0.14 g) and specific heat capacity (2.66 J/(g·℃)) of f-EPx, respectively. Q_s and Q_{loss} represent the energy incident on the sample and dissipated into the air, respectively. When the temperature reaches its equilibrium value, the system is in equilibrium, then:

$$Q_s = Q_{loss} = hS \triangle T_{max} \tag{S2}$$

where h is the heat-transfer coefficient, S is the surface area of sample, and ΔT_{max} is the maximum temperature difference (68.4 ℃). Photothermal conversion efficiency (η_{pt}):[4,5]

$$\eta_{pt} = \frac{hS \triangle T_{max}}{I(1 - 10^{-A_{808}})} \tag{S3}$$

where I is the laser power (1 W), A_{808} is the absorbance at the wavelength of 808 nm (1.36). A dimensionless driving force temperature, θ is introduced to obtain hS:

$$\theta = \frac{\triangle\ T}{\triangle\ T_{max}} \tag{S4}$$

where ΔT is the maximum temperature difference between sample and environment. The sample system time constant τ:

$$\tau = \frac{\sum_i m_i C_{pi}}{hS} \tag{S5}$$

Substituting the above equations into Equation (S3), we get:

$$\frac{d\theta}{dt} = \frac{1}{\tau hS}\frac{Q_s}{\triangle\ T_{max}} - \frac{\theta}{\tau} \tag{S6}$$

After the light irradiation stops, Q_s becomes 0, and Equation (S6) can be rearranged as:

$$t = -\tau \ln \theta \tag{S7}$$

Therefore, the slope of the line obtained by fitting t-(-lnθ) is τ (28.77 s), as shown in Figure 7(d). By substituting Equation (S5) into Equation (S3), the photothermal conversion efficiencies of f-EP6 can be obtained as 92.6%.

Table S1. Name and Formulation of ENR/PANI/$FeCl_3$ composites

Sample	ENR	PANI (phr)	$FeCl_3$ (phr)	DCP (phr)
EP0	100	30	0	0
EP3	100	30	3	0
EP6	100	30	6	0
EP9	100	30	9	0
E6	100	0	6	0
ED	100	0	0	2

Reference

[1] J. Cao, C. Lu, J. Zhuang, M. Liu, X. Zhang, Y. Yu and Q. Tao, Angew. Chem. Int.

Ed., 2017, 56, 8795-8800.

[2] J. Zhu, X. Li, Y. Weng, B. Tan and S. Zhang, J. Supercrit. Fluids, 2022, 181, 105508.

[3] X. Huang, J. Liu, P. Zhou, G. Su, T. Zhou, X. Zhang and C. Zhang, Small, 2022, 18, 2104048.

[4] M. Lahikainen, H. Zeng and A. Priimagi, Nat. Commun., 2018, 9, 1-8.

[5] D. Liu, L. Ma, L. Liu, L. Wang, Y. Liu, Q. Jia, Q. Guo, G. Zhang and J. Zhou, ACS Appl. Mater. Interfaces, 2016, 8, 24455-24462.